Computers and Geosciences 109 (2017) 238–246

Contents lists available at ScienceDirect

Computers and Geosciences

journal homepage: www.elsevier.com/locate/cageo

Research paper

A novel orthoimage mosaic method using the weighted A* algorithm for UAV imagery

Maoteng Zheng [a,*], Shunping Zhou [a], Xiaodong Xiong [b], Junfeng Zhu [b]

[a] National Engineering Research Center for Geographic Information System, China University of Geosciences, Wuhan, China
[b] Mirauge3D Technology Inc., Beijing, China

ARTICLE INFO

Index term:
Orthoimage mosaic
Weighted A* algorithm
Voronoi Diagram
Digital Surface Model
Edge diagram

ABSTRACT

A weighted A* algorithm is proposed to select optimal seam-lines in orthoimage mosaic for UAV (Unmanned Aircraft Vehicle) imagery. The whole workflow includes four steps: the initial seam-line network is firstly generated by standard Voronoi Diagram algorithm; an edge diagram is then detected based on DSM (Digital Surface Model) data; the vertices (conjunction nodes) of initial network are relocated since some of them are on the high objects (buildings, trees and other artificial structures); and, the initial seam-lines are finally refined using the weighted A* algorithm based on the edge diagram and the relocated vertices. The method was tested with two real UAV datasets. Preliminary results show that the proposed method produces acceptable mosaic images in both the urban and mountainous areas, and is better than the result of the state-of-the-art methods on the datasets.

1. Introduction

Nowadays, the UAV images are widely used in digital mapping especially for those areas that are unreachable, for example, the desert, mountains and other dangerous locations. In the UAV mapping process, the source images are firstly rectified to orthoimages based on the corresponding DSM (Digital Surface Model) or DEM (Digital Elevation Model) data, and then these orthoimages are stitched together, forming a large orthoimage. There are, however, seam-lines in the big orthoimage due to the inconsistencies between adjacent small orthoimages in both geometric and radiometric perspectives. The geometric inconsistency is mainly caused by the object's height and the different viewing angles while the radiometric inconformity is affected by the viewing and illumination angles, and different imaging time. A lot of research works have been done to resolve these problems. The research undertaken may be classified into two categories: image-based and ground-based methods. Image-based methods only use the color information to guide the seam-line to avoid areas with large intensity contrast, and make sure that the color difference on the seam-line is minimized. On the other hand, the ground-based methods use the ground information such as DSM, DEM, OESM (Orthoimage Elevation Synchronous Model), LiDAR (Light Detection and Ranging) point cloud and others, to guide the seam-line to avoid high objects (for instance buildings and trees) on the ground.

Image-based methods do not need any ground information, and the only input required is the orthoimage. The color information is used to determine an optimal seam-line which has minimal difference between the adjacent orthoimages (Botterill et al., 2010; Chon et al., 2010; Fernández et al., 1998; Fernández and Martí, 1999; Kerschner, 2001; Mills and McLeod, 2013; Pan et al., 2009, 2014; Soille, 2006; Wan et al., 2012, 2013; Yu et al., 2012; Zagrouba et al., 2009; Zhao et al., 2013). Generally, a cost function is used to represent the difference, and the main objective is to find the optimal seam-line which has the minimal cost. Based on this theory, twin snakes algorithm (Kerschner, 2001), Dijkstra's algorithm (Chon et al., 2010) (Wan et al., 2012, 2013; Dijkstra, 1959; Li et al., 2015), the A* algorithm (Hart et al., 1968), morphological algorithm (Soille, 2006) and other methods are proposed.

As mentioned above, the ground-based methods apply the auxiliary data such as DSM, DEM, OESM, and LiDAR point cloud. With the help of the ground information, the locations of starting and ending points of seam-lines can be adjusted according to the height information, and the optimal seam-line can be extracted by avoiding the high objects (Chen et al., 2014; Ma and Sun, 2011; Pang et al., 2016). The method proposed by Chen et al. (2014) needs both the DSM and DEM data. DEM is the filtering result of DSM (Chen et al., 2014), and the filtering process itself is an immature technique which needs further study. Good DEM data is rarely found especially in the UAV (Unmanned Aircraft Vehicle) mapping

* Corresponding author.
E-mail address: tengve@163.com (M. Zheng).

http://dx.doi.org/10.1016/j.cageo.2017.08.004
Received 22 March 2017; Received in revised form 28 June 2017; Accepted 1 August 2017
Available online 2 August 2017
0098-3004/

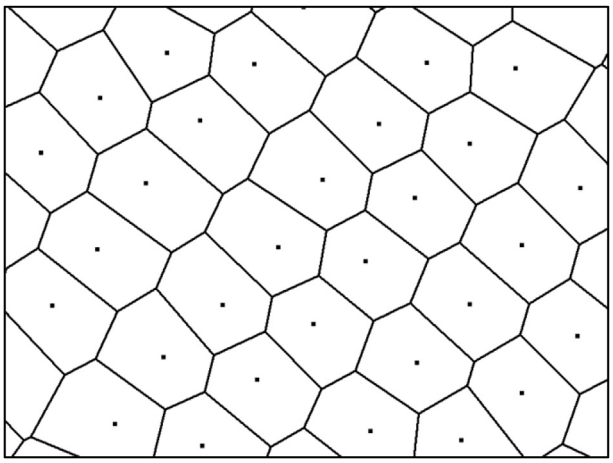

Fig. 1. Voronoi Diagram of a constrained area.

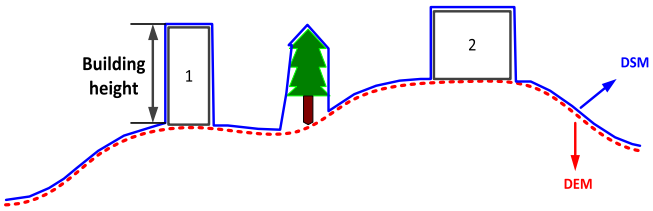

Fig. 2. DSM (solid blue line) and DEM (dashed red line) of the same area. (For interpretation of the references to colour in this figure legend, the reader is referred to the web version of this article.)

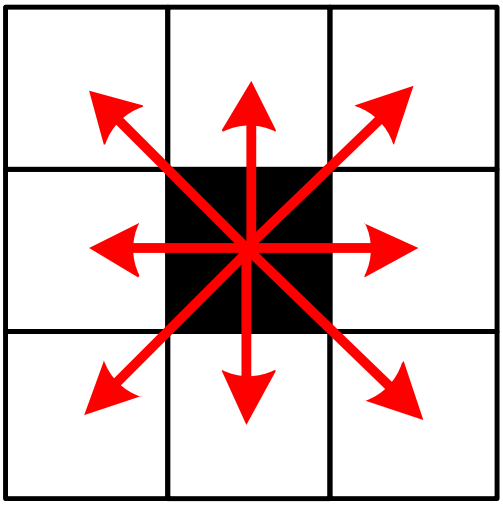

Fig. 3. 8 directions in the neighborhood of a pixel.

application. Ma et al. (2014) used the LiDAR point cloud (Ma and Sun, 2011). However, the filtering of non-ground points in the point cloud is critical. Pang et al. (2016) claimed that no additional data is used, but the exterior orientation parameters were nonetheless used to generate epipolar images and conduct SGM (Semi-Global Matching) (Pang et al., 2016). Their method is still vulnerable when used in mountainous area or UAV images. Furthermore, the above methods did not specify how to adjust the starting points and the ending points of seam-lines when they are located on the building.

These two methods can achieve reasonable results for certain data sources, but neither can deliver perfect result for UAV images. In this paper, the ground data DSM combined with a weighted A* algorithm are applied to search for seam-lines. The A* algorithm is a well-known shortest path-finding algorithm which utilizes the advantages of both Dijkstra's algorithm and Best-First-Search algorithm (Niu and Zhuo, 2008). The standard A* algorithm is improved in this paper, and the height gradient is added to the cost function to refine the seam-lines.

2. Methodology

2.1. Initial seam-line network

To generate a single big orthoimage with a number of small orthoimages, each of the small orthoimage contributes a polygon area of the big mosaic. The boundaries between adjacent orthoimages are called seam-lines. The seam-lines connect to each other to form a seam-line network. Voronoi Diagram algorithm can partition a 2D space to unique small polygons once a group of seed points are given. Each seed point is surrounded by a unique polygon, and all the polygons connected to each other with no overlap form a Voronoi Diagram as shown in Fig. 1. More information about Voronoi Diagram can be found in the reference (Milgram, 1975).

2.2. Seam-line network optimization

After the initial seam-line network is built using Voronoi Diagram, the seam-lines are optimized. Firstly, a height gradient diagram (edge diagram) is generated based on DSM data. Then, a weighted A* algorithm is applied to search for an optimal path which avoids the buildings and other high artificial objects on the image.

2.2.1. Edge diagram generation

To pilot a seam-line to avoid high objects, the heights of artificial objects (buildings, trees and others) should be obtained. It can be calculated by the difference between DSM and DEM as shown in Fig. 2. However, it is impossible to detect the height of high objects solely by using DSM data. Hence Chen et al. (2014) used both the DSM and DEM data.

Nonetheless, the height gradient can be computed using the DSM data. For seam-line selection, if the areas with large height gradient were avoided, the high objects can be avoided. According to this rule, a height gradient diagram should be firstly generated using the DSM data by setting a gradient threshold. The seam-lines can then be refined based on this height gradient diagram. Generally, the DSM file is stored as an image in geotiff format, and the pixel size is the interval of the DSM. The height gradient of a pixel is the maximum height gradient in 8 directions in the 8-neighborhood areas as shown in Fig. 3 and Equation (1).

$$Grad(i,j) = \max(g_1, g_2, g_3, g_4, g_5, g_6, g_7, g_8) \quad (1)$$

where g_k ($k = 0, 1, \ldots 8$) are the height gradients in the 8 directions.

A height gradient diagram which has the same size to the DSM file is partly shown in Fig. 4.

As shown in Fig. 4, the height gradient diagram mainly consists of edges; hence it is called the edge diagram. Once the edge diagram is generated, the whole seam-line network can be optimized based on this diagram. This is different from other methods that determine the seam-line based on the color difference (image-based methods) or the height difference (ground-based method) in the overlap area of the adjacent images. Different seam-lines are determined in different overlap areas. The proposed method directly refines all the seam-lines on a single edge diagram which has the same size to the DSM data of the whole block.

The optimization of seam-line network should include the optimization of vertex locations and the optimization of seam-lines.

2.2.2. Vertex relocation

The initial positions of vertices are unpredictable, for some may be located on the roofs of buildings or on trees. If the locations of those

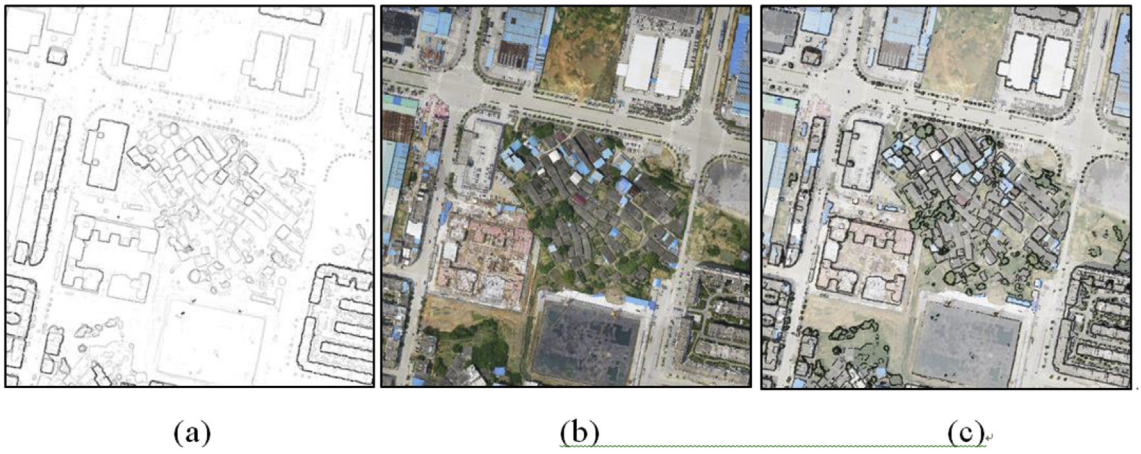

Fig. 4. Image (a) is a part of the edge diagram; (b) is the corresponding image; and (c) is the superposition of (a) and (b).

Fig. 5. A large ground structure in the image. Red lines are initial seam-line network; the vertices (conjunction node) in the image to the left are mostly located on the buildings while the vertices in the image to the right have been moved to near the ground. (For interpretation of the references to colour in this figure legend, the reader is referred to the web version of this article.)

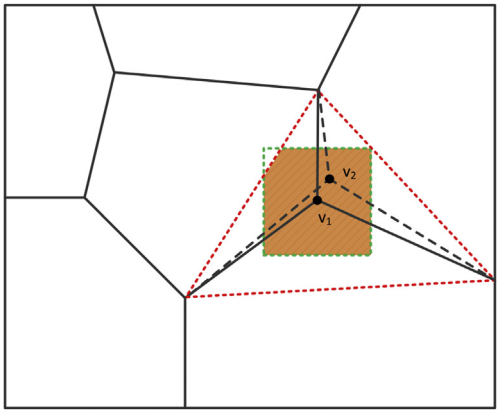

Fig. 6. The combined constrained area (filled area), the intersection of the red dashed triangle and green rectangle. (For interpretation of the references to colour in this figure legend, the reader is referred to the web version of this article.)

vertices are fixed on the roofs, the related seam-lines will definitely cut some buildings. Therefore it is necessary to move those vertices from roofs to locations on the ground. The vertices must however be constrained in a designated region where the vertices can move freely while the topologic characteristic of the initial network is maintained. To accomplish this goal, Mills et al. (Mills and McLeod, 2013) defined a circle region around the vertex as the search region. But the vertices might still located on the buildings since no ground data is used in their method.

In this paper, a new and bigger constrained area is defined. For the networks generated by Voronoi Diagram, the vertices (not located on the border) are always connected by three vertices as shown in Fig. 1. The triangle consists of the three adjacent vertices, and is defined as the constrained area for a vertex. To maintain the network in good shape, a square-shaped constrained area is also defined to prevent the vertex from moving to their neighboring vertices. The size of the square is determined based on the building density in the dataset. It's an empirical value. It's set to 60pixel * 60pixel in this paper. The final constrained area is shown in Fig. 6.

Once the constrained area is defined, the optimal vertex location can be determined by two steps:

1) For every pixel in the constrained area, compute the minimal distance to the nearest edge L_{min}.
2) Find candidate pixels and interpolate their height from DSM data. The candidate pixels must meet the requirement that the $L_{\min}$ value is bigger than a threshold value T_d ($T_d = 5$ pixels in this paper).
3) Select the pixel which has the lowest height from the candidate pixels as the final result.

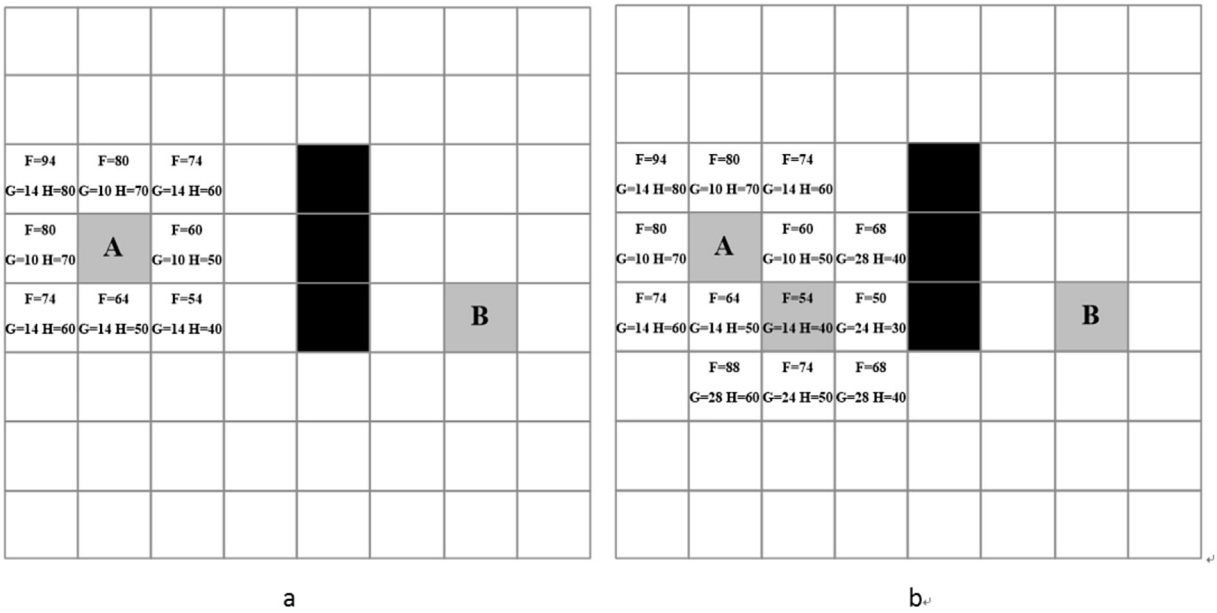

Fig. 7. The first two steps of the A* searching process. Each rectangle represents a pixel in the image. The filled gray rectangle A is the starting point, B is the ending point, and the filled black rectangles in the middle are the obstacle pixels. We assume that the distance between the horizontal and vertical adjacent pixels is 10 units and the distance between the adjacent diagonal pixels is 14 units.

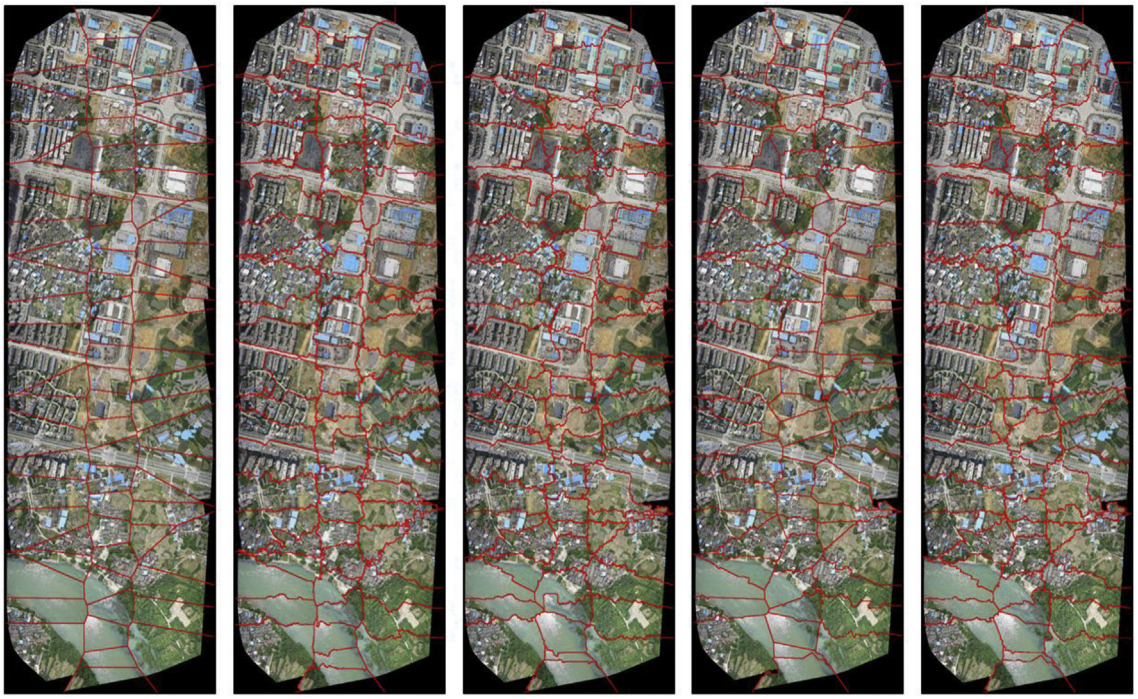

Fig. 8. Comparison of the initial and refined seam-line networks on dataset 1. The images from left to right are the initial seam-line network, the seam-line network refined by Chon's method, VR-Chon's method, the proposed method, and the DSM-Color method respectively. The red lines in the images are seam-lines. (For interpretation of the references to colour in this figure legend, the reader is referred to the web version of this article.)

Steps 1 and 2 ensure that the candidate locations are far away from the edges (buildings). Step 3 makes sure that the locations are moved off the roof since the height of the roof is much larger than the ground points in the constrained area. The size of square region and the threshold T_d are both related to the building density on the ground. The result of vertex relocation is shown in Fig. 5. If there are dense buildings in the constrained area, the algorithm will failed to find a ground point; the vertex will stay on the building.

2.2.3. *The weighted A* algorithm*

To bypass the high objects using the edge diagram. A weighted A* algorithm is introduced to accomplish this job.

The A* algorithm was firstly proposed by Peter E. Hart (Hart et al., 1968) to search for a minimum cost path in 1968. It is a graph searching algorithm (Kim et al., 2015). The mathematical basis of this algorithm can be found in the original paper (Hart et al., 1968). The cost function is written as follows:

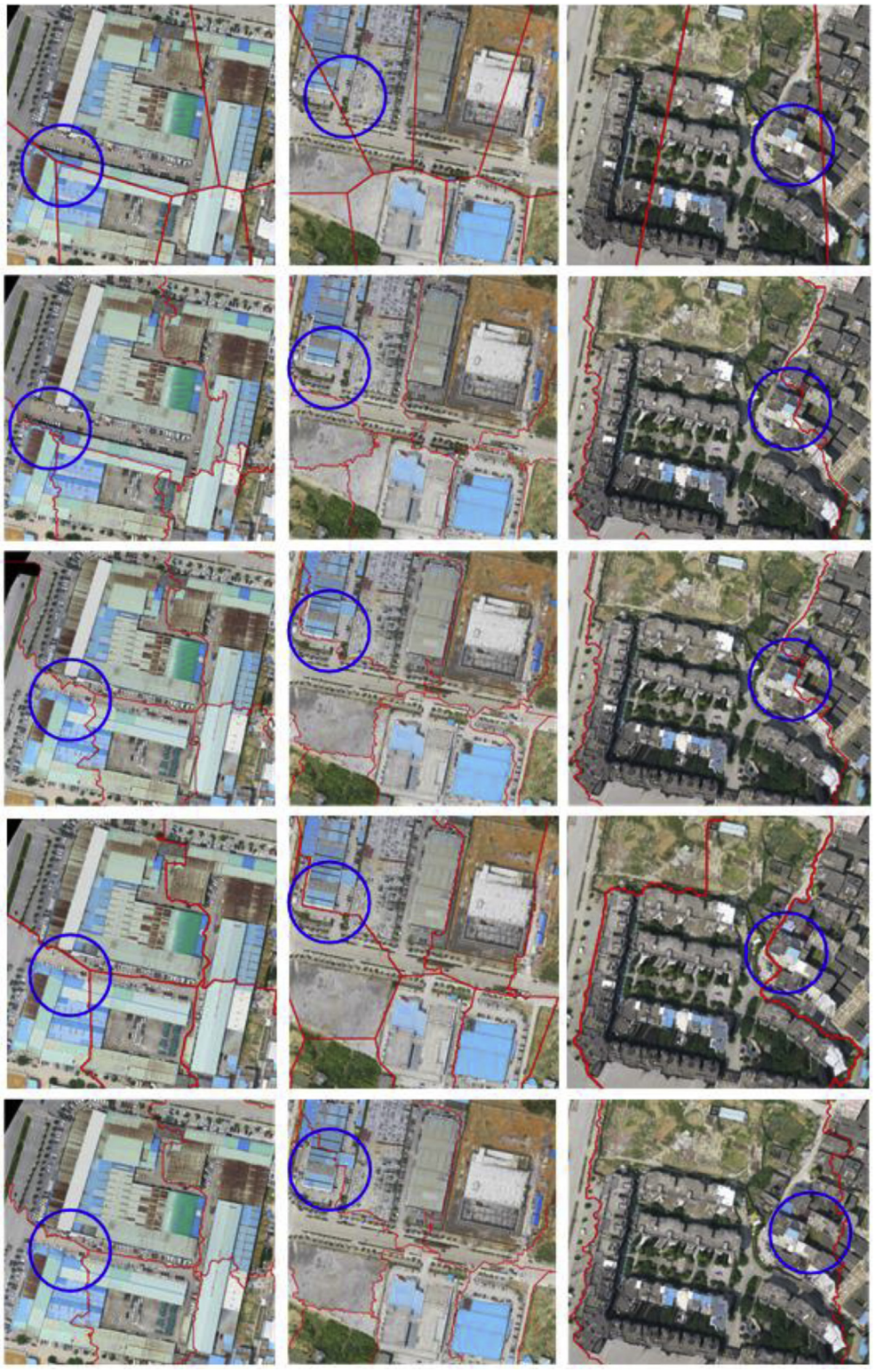

Fig. 9. Comparison of initial seam-lines and the optimized seam-lines with the dataset 1 in details. The five rows of images from top to bottom show the initial seam-lines, the seam-lines refined by Chon's method, VR-Chon's method, the proposed method, and the DSM-Color method respectively. The blue circles mark the main differences of different methods. (For interpretation of the references to colour in this figure legend, the reader is referred to the web version of this article.)

$$F = G + H \tag{3}$$

where F is the total cost moving from the starting point through the current point to the ending point; G is the movement cost from the starting point to the current point; and H is the estimated movement cost from the current point to the ending point.

As can be seen in Fig. 7a, the adjacent pixel where F = 54 has the least cost among the 8 neighborhood of start point A. So it is selected for the starting point of the next step as shown in Fig. 7b. The estimated movement cost function H actually has multiple choices (Hart et al., 1968). In this paper, we define H as the Manhattan Distance from the

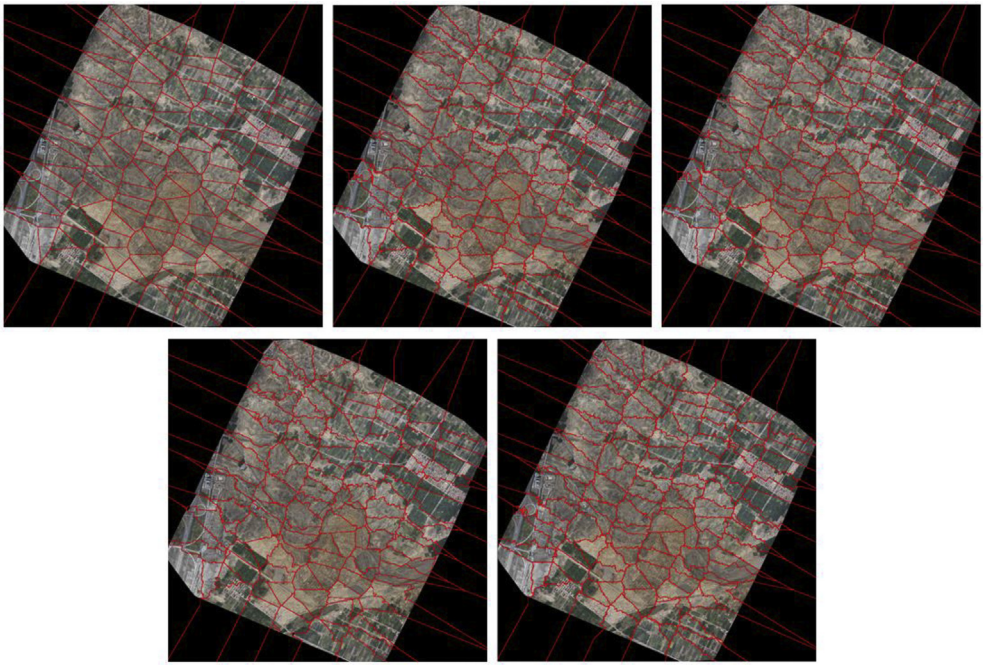

Fig. 10. Comparison of initial and refined seam-lines. The three images on the top from left to right show the initial seam-line network, the seam-line network refined by Chon's method and VR-Chon's method respectively. The two images on the bottom show the seam-line network refined by the proposed method and the DSM-Color method respectively. (For interpretation of the references to colour in this figure legend, the reader is referred to the web version of this article.)

current point to the ending point. Its role in the A* algorithm is to make sure the searching process is converging to the ending point. As can be seen in Equation (3), when the searching process is getting closer to the ending point, H function is decreasing, and the cost function is decreasing. In the contrast, when the searching process is getting farther, H function is increasing, and the cost function is increasing. Since we are choosing the path where the cost function is minimal, the H function can actually make sure the A* algorithm will eventually converge to the ending point. We only present the first two steps here; the detailed searching process is much more complex, and it can be found in (Hart et al., 1968; Amit, 2016; Lester, 2017).

For the orthoimage mosaic, the seam-lines are expected to be the shortest paths and have minimal geometric and radiometric differences. In this paper, only the geometric inconsistence is explored. To diminish the geometric difference, the seam-line has to avoid high objects. In other words, a good seam-line should avoid the areas with large height gradient. Thus, we can modify the cost function in Equation (3) and create a new one as shown in Equation (4).

$$F_w = \alpha^*(G+H) + \beta^*X \tag{4}$$

where F_w is the new cost function; the term X is a measurement which reflects the geometric inconsistency along the seam-line; the two variables $\alpha \in [0,1]$ *and* $\beta \in [0,1]$ are the coefficients of $G+H$ and X respectively.

There are multiple choices for the term X. For an instance, we can choose the height gradient.

$$X = \begin{cases} 0 & Grad < T_G \\ k_G{}^*Grad & Grad \geq T_G \end{cases} \tag{5}$$

where T_G is a threshold value for height gradient, k_G is a positive coefficient converting the height gradient to term X. In this paper, k_G is set to 20.

The coefficient T_G is used to identify the flat area. If the height gradient of the pixel is smaller than T_G, then we can define the pixel as flat area. In this paper, the value of T_G is set to 0.5 m. It means that the area with height difference smaller than 0.5 m is treated as a plane area with zero height gradient.

Actually, the color difference can be also chosen as the term X. If only color difference is used, the method is similar with other image-based methods. Then the term X can be computed as follows:

$$dI = I_l - I_r \tag{6}$$

where dI is the color difference of the conjugate points on adjacent orthoimages, the intensity of the point on the left orthoimage is I_l, and the intensity of the corresponding point on the right orthoimage is I_r.

$$X = \begin{cases} 0 & dI < T_I \\ k_I{}^*dI & dI \geq T_I \end{cases} \tag{7}$$

where T_I is a threshold value for color difference, k_I is a positive coefficient converting the color difference to term X.

A combination of both height gradient and color difference will also work. Then the term X can be computed as follows:

$$X = \begin{cases} 0 & dI < T_I \;\&\&\; Grad < T_G \\ k_G{}^*Grad + k_I{}^*dI & Others \end{cases} \tag{8}$$

Multiple choices are available for the term X, but we use only height gradient in this paper. The proposed method is based on DSM data only. However, the DSM (provide height gradient) plus color (provide color difference) based method is also tested and compared in the experiment.

For simplicity, Equation (4) is rewritten as follows:

$$F_w = \alpha^*D + \beta^*X \tag{9}$$

where $D = G+H$ is the path length term.

If $\alpha = 1$ and $\beta = 0$, then Equation (5) is a standard A* cost function, and the seam-line will be a straight line from the starting point to the ending point. The value of α must be bigger than zero since the path length term D makes sure the searching process is approaching the ending point. If $\beta \neq 0$, the height gradient will contribute to the cost function with a factor of β, and the cost function will force the seam-line to avoid the areas with large height gradient. In this paper, none-obstacle area is set in the orthoimage, but the height gradient term X will make

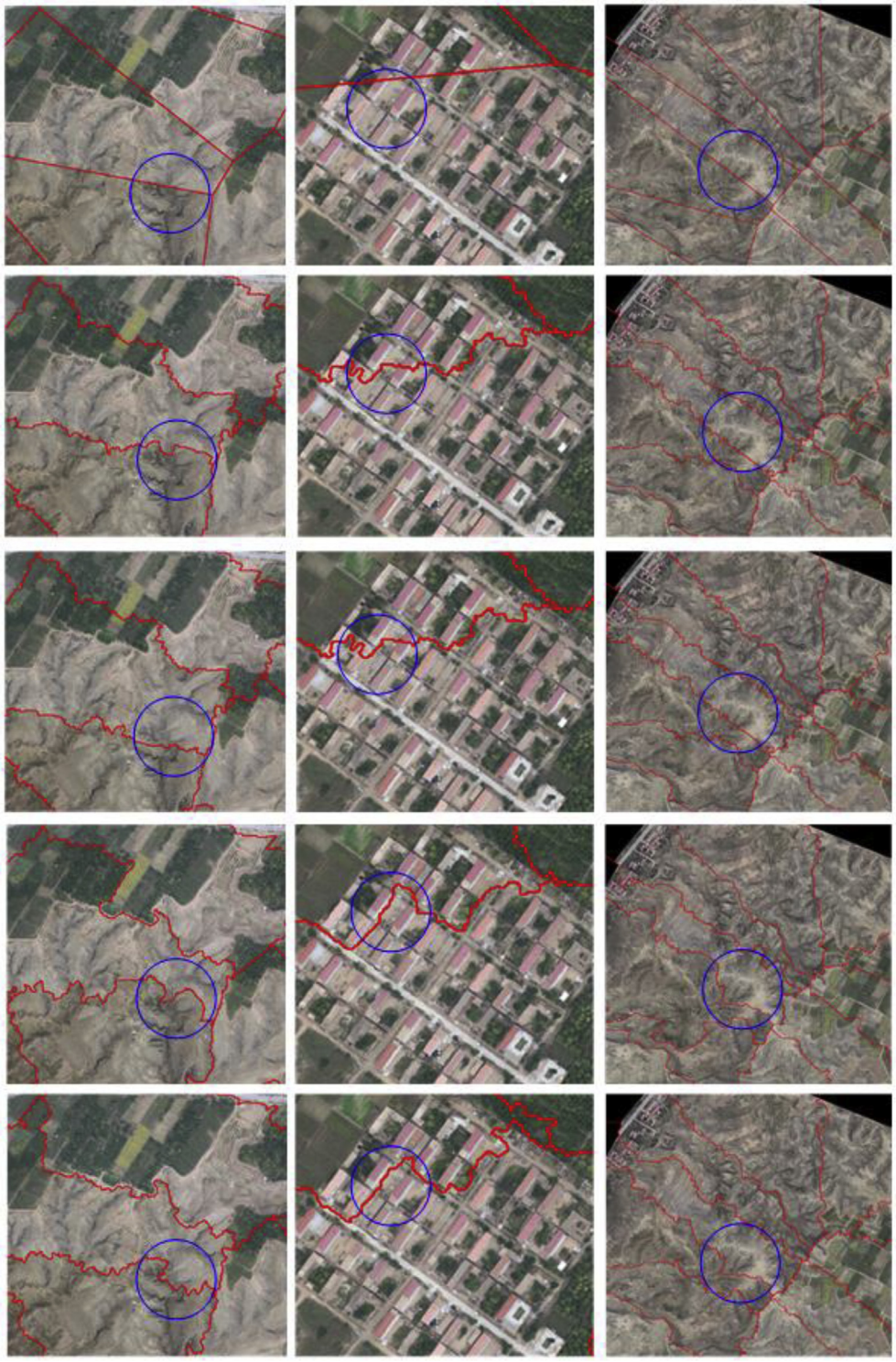

Fig. 11. Comparison of the initial seam-lines and the optimized seam-lines with test dataset 2 in details. The five rows of images represent the initial seam-lines, the seam-lines refined by Chon's method, VR-Chon's method, the proposed method and the DSM-Color method respectively. The blue circles mark the main differences of different methods. (For interpretation of the references to colour in this figure legend, the reader is referred to the web version of this article.)

sure the searching process will bypass higher objects (buildings). The values of α and β can also be referred to the weights of the path length and height gradient in the new cost function respectively, hence we call it the weighted A* algorithm.

There is a tradeoff between the shortest path and smallest height gradient controlled by the two coefficients α and β. If $\alpha > \beta$, the searched path should be shorter and more like a straight line; if $\alpha < \beta$, the searched path will avoid higher objects and may be curved and longer. The value of α and β should be determined according to the real dataset (Terrain type, building density, and so on). In this paper, we choose $\alpha = 0.3$ and $\beta = 0.6$.

3. Experiment and analysis

3.1. Dataset

To fully evaluate the proposed method, two datasets of UAV images

Table 1
Description of experiment schemes.

Scheme	Description
Chon's method	Pure Chon's method as described in his paper
VR-Chon's method	A combined method of vertex relocation and Chon; s method. Firstly, vertex relocation algorithm as described in Section 2.2.(b) are applied to refine vertex location of the seam-line network, then Chon's method are used to refine seam-lines
Proposed method(DSM)	The proposed method using only DSM data
DSM-Color method	The proposed method using both DSM and color information

are tested. They include 75 and 120 orthoimages respectively. The GSD (Ground Sampling Distance) of the first dataset is 0.24 m and the ground coverage of each orthoimage is about 320*430 m^2. The GSD of the second dataset is 0.35 m and the ground coverage of each orthoimage is about 1189*1035 m^2. The DSM used in this paper is extracted from the raw images of these two datasets using the SGM algorithm (Pang et al., 2016). The grid interval of DSM is 0.5 m * 0.5 m. An ortho rectification and mosaic program was developed by the authors according to the above methods.

3.2. Experiment scheme and environment

Four different methods are tested with the above datasets. They are Chon's method (Chon et al., 2010), an advanced Chon's method (Vertex relocation combined with Chon's method), proposed method using only DSM and proposed method using both DSM and color information. For the DSM and color based method, threshold T_I is set to 10, the coefficients k_G and k_I are both set to 20 in Equation (8). All the experiments were conducted on a common computer equipped with the Inter (R) Core(TM) i5-33320M 2.60 GHz CPU, 8.00 GB RAM, and 64bit Window 7 Operating System.

3.3. Results and analysis

The initial network was firstly generated by Voronoi Diagram algorithm, and then refined by Chon's method, VR-Chon's method, the proposed method and the DSM-Color method respectively (see Table 1). The initial and refined networks of the two datasets are shown in Figs. 8–11. The processing time of the whole procedure of each method is also recorded and listed in Table 2.

For dataset 1, some vertices of the initial seam-line network are located on the buildings as shown in the left top image in Fig. 9. Most of the initial seam-lines cut buildings as demonstrated in the three images at the top. Chon's method can improve the seam-line network to some extent, but the vertices locations are not refined since they didn't apply any vertex relocation algorithm. When the vertex relocation algorithm as introduced in this paper is combined with Chon's method, most of the vertices located on the buildings are moved to the near ground, and better seam-lines are obtained compared to pure Chon's method as shown in the two and third row of Fig. 9. However, VR-Chon's method still cut some buildings while the proposed method can successfully pilot the seam-lines to bypass the buildings as shown in the right images on row 3 and 4 in Fig. 9. The seam-lines refined by VR-Chon's method are also more curved than the proposed method. For the DSM-Color method, it does not produce better results than the proposed method, the seam-lines are also more curved, and some seam-lines still cut buildings while the seam-line refined by the proposed method don't.

Table 2
Comparison of different algorithms.

Methods	Dataset1 (flat area)		Dataset2 (mountain area)	
	Processing time (seconds)	Number of buildings cut through by seam-lines	Processing time (seconds)	Number of buildings cut through by seam-lines
Initial network	/	221	/	45
Chon's method	326	161	317	24
VR-Chon's method	313	131	316	20
Proposed method (DSM)	**108**	**71**	**219**	**3**
DSM-Color method	286	125	362	12

The above analysis can be also verified by the quantitative results as listed in Table 2. Chon's method cut less buildings compared to initial seam-lines, and VR-Chon's method can do better than Chon's method but worse than the proposed method. Chon's method with or without vertex relocation need more time to complete the job compared to the proposed method. In a word, the proposed method is the most efficient compared to the other three.

In dataset 2, the ground coverage is a small mountainous area. Some initial seam-lines cross the artificial buildings (low houses) as shown in the top images in Fig. 11, and some also cross the mountain peaks which is undesirable for orthoimage mosaic. The refined seam-lines are expected to go through areas where the height gradient is zero or very small (smooth area in height). As can be seen in the second row in Fig. 11, the seam-lines refined by Chon's method and VR-Chon's method go through some mountain peaks. They also cut some houses. But for the proposed method, the seam-lines in the mountain area mostly go smoothly around the mountain peaks. The seam-lines avoid most of the low houses as they did in dataset 1. As the same as the test result for dataset 1, the propose method produce the best results than the other three methods. The above analysis is also verified by the quantitative results shown in Table 2.

4. Conclusion

This paper introduced a novel orthoimage mosaic method based on the proposed weighted A* algorithm. The whole workflow includes 4 steps: generation of initial seam-line network by standard Voronoi Diagram algorithm, generation of edge diagram based on DSM data, relocation of vertices based on edge diagram, and optimization of seam-lines using weighted A* algorithm based on new vertex locations and the edge diagram. The proposed method was tested using two real datasets of UAV images. Total 4 methods: Chon's method (Chon et al., 2010), VR-Chon's method, propose method using only DSM and proposed method using both DSM and color are compared and analyzed. Based on the results of experiments, we can conclude that:

1) The proposed method is suitable for UAV images in both urban and mountainous areas, and it can produce acceptable big mosaic orthoimage automatically.
2) The vertex relocation algorithm is useful since VR-Chon's method can produce better result than Chon's method.
3) The proposed method using only DSM produces better results than both Chon's method and VR-Chon's method. It's also better than the proposed method using both DSM and color.
4) The proposed method using only DSM is a global solution. Vertex relocation and seam-line optimization are all processed based on a single edge diagram generated by the DSM.

With different terms combined in the cost function, the proposed method can search different optimal paths in different perspectives such as color difference, traffic congestion, road price and others. If the traffic congestion term is combined in the cost function, a path with minimal traffic jam can be selected. For orthoimage mosaic, more tests with real datasets are still needed to verify the robustness of the proposed method. We have to admit that the outcome of the proposed method is highly

related to the quality of the DSM. The higher the quality of the DSM, the better the mosaic. If the DSM cannot reflect the real surface, the resultant seam-line network will be compromised.

Acknowledgements

This project is funded by the National Natural Science Foundation of China under grant 41601502, China Postdoctoral Science Foundation under grant 2015M572224, and the Fundamental Research Funds for the Central Universities, China University of Geosciences (Wuhan) under grants CUG160838 and CUG170664.

References

Amit, Amit's Game Programming Information. http://www-csstudents.stanford.edu/~amitp/gameprog.html. (Accessed 08 November 2016).
Botterill, T., Mills, S., Green, R., 2010. Real-time aerial image mosaicing. In: Proceedings of the IEEE International Conference of Image and Vision Computing New Zealand, Queenstown, New Zealand, pp. 8–9 (November).
Chen, Q., Sun, M., Hu, X., Zhang, Z., 2014. Automatic seamline network generation for urban orthophoto mosaicking with the use of a digital surface model. Remote Sens. 6, 12334–12359.
Chon, J., Kim, H., Lin, C., 2010. Seam-line determination for image mosaicking: a technique minimizing the maximum local mismatch and the global cost. ISPRS J. Photogramm. Remote Sens. 65, 86–92.
Dijkstra, E.W., 1959. A note on two problems in connexion with graphs. Numer. Math. 1, 269–271.
Fernández, E., Martí, R., 1999. GRASP for seam drawing in mosaicking of aerial photographic maps. J. Heuristics 5, 181–197.
Fernández, E., Garfinkel, R., Arbiol, R., 1998. Mosaicking of aerial photographic maps via seams defined by bottleneck shortest paths. Oper. Res. 46, 293–304.
Hart, P.E.G., Nilsson, N.J., Raphael, B., 1968. A formal basis for the heuristic determination of minimum cost paths. IEEE Trans. Syst. Sci. Cybern. SSC4.
Kerschner, M., 2001. Seamline detection in colour orthoimage mosaicking by use of twin snakes. ISPRS J. Photogramm. Remote Sens. 56, 53–64.
Kim, K.H., Sin, S., Lee, W., 2015. Exploring 3D shortest distance using a* algorithm in Unity3D. J. Arts Imaging Sci. 2 (3), 1–5.
Lester P., A* Pathfinding for Beginners, http://www.policyalmanac.org/games/aStarTutorial.htm. (Accessed 12 March 2017).
Li, X., Hui, N., Shen, H., et al., 2015. A robust mosaicking procedure for high spatial resolution remote sensing images. ISRPS J. Photogram. Remote Sens. 109, 108–125.
Ma, H., Sun, J., 2011. Intelligent optimization of seam-line finding for orthophoto mosaicking with LiDAR point clouds. J. Zhejiang Univ. Sci. 12, 417–429.
Milgram, D.L., 1975. Computer methods for creating photomosaics. IEEE Trans. Comput. 24, 1113–1119.
Mills, S., McLeod, P., 2013. Global seamline networks for orthomosaic generation via local search. ISPRS J. Photogramm. Remote Sens. 75, 101–111.
Niu, L., Zhuo, G., 2008. An improved real 3D A* algorithm for difficult path finding situation. Int. Archiv. Photogram., Remote Sens. Spatial Inf. Sci. XXXVII (Part B4), 927–930.
Pan, J., Wang, M., Li, D., Li, J., 2009. Automatic generation of seamline network using area Voronoi diagrams with overlap. IEEE Trans. Geosci. Remote Sens. 47, 1737–1744.
Pan, J., Zhou, Q., Wang, M., 2014. Seamline determination based on segmentation for urban image mosaicking. IEEE Geosci. Remote Sens. Lett. 11, 1335–1339.
Pang, S., Sun, M., Hu, X., Zhang, Z., 2016. SGM-based seamline determination for urban orthophoto mosaicking. ISPRS J. Photogramm. Remote Sens. 112 (2016), 1–12.
Soille, P., 2006. Morphological image compositing. IEEE Trans. Pattern Anal. Mach. Intell. 28, 673–683.
Wan, Y., Wang, D., Xiao, J., Wang, X., Yu, Y., Xu, J., 2012. Tracking of vector roads for the determination of seams in aerial image mosaics. IEEE Geosci. Remote Sens. Lett. 9, 328–332.
Wan, Y., Wang, D., Xiao, J., Lai, X., Xu, J., 2013. Automatic determination of seamlines for aerial image mosaicking based on vector roads alone. ISPRS J. Photogramm. Remote Sens. 76, 1–10.
Yu, L., Holden, E.J., Dentith, M.C., Zhang, H., 2012. Towards the automatic selection of optimal seam line locations when merging optical remote sensing images. Int. J. Remote Sens. 33, 1000–1014.
Zagrouba, E., Barhoumi, W., Amri, S., 2009. An efficient image-mosaicing method based on multifeature matching. Mach. Vis. Appl. 20, 139–162.
Zhao, Y., Han, T., Feng, S., et al., 2013. Remote sensing image mosaic by incorporating segmentation and the shortest path. Commun. Comput. Inf. Sci. 398, 684–691.